Research Paper

DCC gene network in the prefrontal cortex is associated with total brain volume in childhood

Alice Morgunova, BA; Irina Pokhvisneva, MSc; Saara Nolvi, PhD; Sonja Entringer, PhD; Pathik Wadhwa, MD, PhD; John Gilmore, MD; Martin Styner, MSc, PhD; Claudia Buss, PhD; Roberto Britto Sassi, MD; Geoffrey B.C. Hall, MSc, PhD; Kieran J. O'Donnell, PhD; Michael J. Meaney, PhD; Patricia P. Silveira, MD, MSc, PhD; Cecilia A. Flores, MSc, PhD

Background: Genetic variation in the guidance cue *DCC* gene is linked to psychopathologies involving dysfunction in the prefrontal cortex. We created an expression-based polygenic risk score (ePRS) based on the *DCC* coexpression gene network in the prefrontal cortex, hypothesizing that it would be associated with individual differences in total brain volume. **Methods:** We filtered single nucleotide polymorphisms (SNPs) from genes coexpressed with *DCC* in the prefrontal cortex obtained from an adult postmortem donors database (BrainEAC) for genes enriched in children 1.5 to 11 years old (BrainSpan). The SNPs were weighted by their effect size in predicting gene expression in the prefrontal cortex, multiplied by their allele number based on an individual's genotype data, and then summarized into an ePRS. We evaluated associations between the *DCC* ePRS and total brain volume in children in 2 community-based cohorts: the Maternal Adversity, Vulnerability and Neurodevelopment (MAVAN) and University of California, Irvine (UCI) projects. For comparison, we calculated a conventional PRS based on a genome-wide association study of total brain volume. **Results:** Higher ePRS was associated with higher total brain volume in children 8 to 10 years old ($\beta = 0.212$, $p = 0.043$; $n = 88$). The conventional PRS at several different thresholds did not predict total brain volume in this cohort. A replication analysis in an independent cohort of newborns from the UCI study showed an association between the ePRS and newborn total brain volume ($\beta = 0.101$, $p = 0.048$; $n = 80$). The genes included in the ePRS demonstrated high levels of coexpression throughout the lifespan and are primarily involved in regulating cellular function. **Limitations:** The relatively small sample size and age differences between the main and replication cohorts were limitations. **Conclusion:** Our findings suggest that the *DCC* coexpression network in the prefrontal cortex is critically involved in whole brain development during the first decade of life. Genes comprising the ePRS are involved in gene translation control and cell adhesion, and their expression in the prefrontal cortex at different stages of life provides a snapshot of their dynamic recruitment.

Introduction

The prefrontal cortex (PFC) modulates executive functions such as attention, decision-making and cognitive control.[1] The maturation of these behaviours parallels the structural refinement of the PFC, including the ingrowth of mesocortical dopamine axons, which continues until early adulthood.[2–11] The gradual maturational trajectory of mesocortical dopamine connectivity — and of the PFC itself — is controlled by the guidance cue Netrin-1 and its receptor DCC, which determine the spatiotemporal targeting of growing axons.[10,12] Studies in rodents show that variations in *Dcc* gene expression lead to differences in cognitive flexibility, behavioural inhibition, vulnerability to stress-induced depression-like behaviours and altered sensitivity to drugs of abuse.[10,11,13–18]

In humans, an autosomal-dominant *DCC* mutation results in structural and functional alterations in the connectivity of mesocortical pathways, with an associated decrease in novelty-seeking behaviour and cigarette use.[19,20] An increasing number of meta-analyses of genome-wide association studies and postmortem human studies have shown that altered levels of *DCC* expression and the presence of specific genetic polymorphisms in the *DCC* gene are associated with psychiatric conditions,[21] most notably major depressive disorder,[15,17,22–35] schizophrenia[34,36–38] and drug abuse.[19,39–42] A study by the Cross-Disorder Group of the Psychiatric Genomics Consortium[3] revealed that a PFC-enriched network of genes prominently affected 8 psychiatric disorders, and a *DCC* single nucleotide polymorphism (SNP) showed the highest pleiotropic association with all 8 disorders. A separate analysis of integrated multi-omics data on genes expressed in the dorsolateral PFC singled out *DCC* as a predictor of well-being, cognitive function and neuroticism.[43] The converging evidence suggests that *DCC* expression in the PFC is critical for neurodevelopment.

In this study, we went beyond investigating genetic mutations or the contributions of SNPs to particular traits, addressing whether variations in the function of the *DCC* gene network in the PFC were associated with differential brain development in children from community-based samples. We used data from well-established child cohorts — the Maternal Adversity, Vulnerability and Neurodevelopment (MAVAN) study[44] and the University of California, Irvine (UCI) project[45,46] — and assessed general brain development, represented by total brain volume. Brain volume measures in children are associated with future cognitive outcomes[47–49] and were used in the present study as an indicator of prominent neurodevelopmental differences.

Methods

MAVAN cohort

Sample

We used data collected from a community-based birth cohort as part of the MAVAN project,[44] for which pregnant women 18 years of age or older were recruited in Montréal (Quebec) and Hamilton (Ontario), Canada. Magnetic resonance imaging of the brain was acquired when the children were 8 to 10 years of age.

Genotyping

As described elsewhere,[50] autosomal SNPs were genotyped from 200 ng of genomic DNA derived from buccal epithelial cells according to manufacturer guidelines, using genome-wide platforms (PsychArray/PsychChip, Illumina). Participant samples with a low call rate (< 90%) were removed, as well as SNPs with a low call rate (< 95%), a minor allele frequency less than 5% or a Hardy–Weinberg equilibrium test $p < 1 \times E^{-40}$, resulting in 260 participants and 242 211 SNPs. We used PLINK 1.9[51] for quality control procedures. The remaining SNPs were submitted for imputation to Sanger Imputation Service using a Haplotype Reference Consortium

(release 1.1) panel[52] and post-imputation quality control, resulting in 20 790 893 SNPs with imputation accuracy greater than 0.80. We recoded imputed dosage genotypes to hard-called genotypes using posterior genotype probability greater than 0.90. Polygenic scores were calculated based on hard-called genotypes.

Because participants were from heterogeneous backgrounds (classified as population stratification), which could have brought bias to genetic associations, we examined population structure using principal component analysis.[53,54] Genotyped SNPs with high linkage disequilibrium ($r^2 < 0.20$) were pruned with a sliding window of 50 kilobases in increments of 5 using PLINK 1.9. We performed principal component analysis using SMARTPCA[53] on this pruned data set and generated a scree plot. Based on the inspection of the scree plot, the first 3 principal components were the most informative of population structure and were included in all analyses as covariates.

Neuroimaging

We used high-resolution T_1-weighted neuroimaging scans and processed them using Multiple Automatically Generated Templates Brain Segmentation Algorithm (MAGeTbrain).[55,56] Scans containing obvious artifacts (such as ghosting or blurring due to head motion) were excluded. Each participant's structural scan was segmented into grey matter, white matter and cerebrospinal fluid. Grey matter and white matter were used to calculate total brain volume.

Replication cohort: University of California Irvine

Sample

We used a prospective, longitudinal study of pregnant mothers and their offspring conducted in the Development, Health and Disease Program[45,46] at the University of California, Irvine (UCI), as a replication cohort. Mothers were recruited during early pregnancy, and shortly after birth their newborns underwent an MRI brain scan during natural, unsedated sleep (postnatal age at scan, mean ± standard deviation 27 ± 13 days).

Genotyping

We used the HumanOmniExpress BeadChip (Illumina) to describe genetic variation in our replication cohort. We performed quality control, imputations, hard-calling and principal component analysis using the same pipelines as for the MAVAN cohort. We performed quality control of the genotype data using PLINK 1.9,[51] removing samples with a low call rate and variants with a low call rate (< 95%), minor allele frequency less than 5% or Hardy–Weinberg equilibrium test $p < \times E^{-25}$. A total of 584 711 genotypes and 142 samples passed quality control. We used the Sanger Imputation Service to impute missing genotypes using the Haplotype Reference Consortium (release 1.1) panel.[52] Following post-imputation quality control and applying an imputation accuracy score of 0.80, 25 060 157 SNPs were left for the downstream analyses. Similar to MAVAN, we recoded imputed dosage genotypes (posterior genotype probability above 0.90)

and used hard-called genotypes for polygenic scores. We applied principal component analysis to the pruned data set to describe population stratification in the UCI cohort and included the first 3 principal components in data analyses of this cohort.

Imaging and MRI acquisition
Infants were scanned using a Siemens 3.0 T Scanner (TIM Trio, Siemens Medical Systems Inc.) as previously described.[45,57] Tissue segmentation was performed using a neonate multi-atlas-based (www.nitrc.org/projects/unc_brain_atlas/), iterative expectation maximization segmentation algorithm as in previous studies from the same cohort.[57] Brain tissue was classified as grey matter, white matter and cerebrospinal fluid. Grey matter and white matter were used to calculate total brain volume, and all 3 tissue types were used to calculate intracranial volume, which was controlled for in the analyses.

Ethics

All clinical and neuropsychological assessments were conducted in accordance with the approvals of the relevant ethics committees for the 3 sites at which the data were collected: 2 sites for MAVAN (Montréal and Hamilton approval for the MAVAN project from McGill University, Université de Montréal, Royal Victoria Hospital, Jewish General Hospital, Centre hospitalier de l'Université de Montréal, Hôpital Maisonneuve-Rosemount, St. Joseph's Hospital and McMaster University) and 1 site for the replication cohort (UCI), for which the UCI institutional review board approved all assessments. All participants' parents provided written informed consent.

Polygenic expression score

Following the protocol described by Silveira and colleagues[50] and Hari Dass and colleagues,[58] we created our expression-based polygenic risk score (ePRS) for the *DCC* coexpression network using brain region and age specificity from publicly available gene expression databases and genotypes from the 2 prospective cohorts. We obtained a list of genes coexpressed with *DCC* in the human adult PFC (absolute correlation of 0.5 or more) from the BrainEAC database (www.braineac.org). Then, we filtered this list to genes that are differentially expressed in children 1.5 to 11 years old compared to adults using data from BrainSpan (www.brainspan.org) by combining the dorsolateral PFC, ventrolateral PFC, medial PFC and orbitofrontal cortex. The resulting list comprised 175 genes; we screened it using the National Center for Biotechnology Information tool to identify annotated SNPs in humans (www.ncbi.nlm.nih.gov/variation/view). We subjected the resulting SNPs to linkage disequilibrium clumping ($r^2 > 0.2$) to yield a list of independent SNPs that were representative of the region. Then, based on the genotype data, we used the count function of the number of alleles at a given SNP and weighed it by the slope coefficient from the GTEx regression model that predicted gene expression in the PFC tissue by

genotype (www.gtex portal.org/home). As such, we calculated the ePRS as the sum of the number of effect alleles multiplied by the effect size of the association between the genotype at a given SNP and the gene expression.

Gene ontology enrichment analysis

To understand the biological functions of the 175 genes that comprised our score, we performed gene ontology enrichment analysis using MetaCore (Clarivate Analytics), a commercially available literature database that screens for main functional networks.

Gene-expression developmental trajectory

To map the *DCC* coexpression network for different developmental periods, we plotted coexpression levels in the PFC in the 4 selected regions (dorsolateral PFC, ventrolateral PFC, medial PFC, orbitofrontal cortex) based on available postmortem data (BrainSpan): childhood ranged from 4 months to 8 years ($n = 11$); adolescence from 11 to 18 years ($n = 4$); and adulthood from 21 to 40 years ($n = 6$). We created a gene-expression correlation matrix for each developmental stage and plotted the resulting data using the heatmaply package.[59] We ordered genes in a consistent manner across time points (based on the correlation matrix calculated for childhood; the order was repeated for the other stages) to help visualize changes in coexpression over time.

Comparison of the *DCC* ePRS with a conventional polygenic risk score for brain volume
Unlike ePRS, which takes into account the fact that co-expressed genes are part of the same network, conventional polygenic risk scores (PRSs) are widely used in population genetics to describe the cumulative, additive effects of a large number of SNPs and their contribution to variation in complex phenotypes,[60] including psychiatric disorders.[61] To identify whether a conventional brain volume PRS would also be associated with total brain volume differences in the MAVAN sample, we calculated PRSs using our accelerated pipeline[62] (https://github.com/MeaneyLab/PRSoS). We created PRSs for each participant based on a meta-analysis of brain volume genome-wide association studies.[63] The data from the genome-wide association studies were created based on the UK Biobank, Enhancing NeuroImaging Genetics through Meta-Analysis partnered with Cohorts for Heart and Aging Research in Genomic Epidemiology (CHARGE), and Early Growth Genetics consortia. We used cumulative summary scores, computed as the sum of the allele count weighted by the effect size described in the meta-analysis[63] across SNPs at different *p* value thresholds.

Statistical analysis

In all analyses, we used the ePRS as a continuous variable to examine its main effect on total brain volume. For the descriptive statistics, we compared children with high and low genetic scores (defined by a median split) on the main confounders.

We used SPSS Inc. (version 20.0–25.0; IBM) and R (R Core Team, 2019) for data analysis. Findings were considered to be statistically significant at $p < 0.05$. We used a Student t test and χ^2 tests to compare baseline characteristics. We performed linear regression analysis to investigate the association between genetic score (*DCC* ePRS) and total brain volume. We considered well-established variables that affect child neurodevelopment as possible confounders. For the MAVAN cohort, we adjusted the model using age at scan, sex, z-score body mass index, principal components and site (Montreal or Hamilton). Because the UCI replication cohort consisted of newborns, we used pediatric age, birth weight ratio,[64,65] sex, intracranial volume and principal components to adjust the model. We corrected the UCI cohort for intracranial volume to account for head size; we did not include this analysis for the MAVAN cohort because intracranial volume and total brain volume were highly correlated in the sample, and adjusting for intracranial volume would have posed a collinearity issue, inflating the variance. We defined pediatric age as age at scan corrected by gestational age at birth.

Results

Dynamic DCC *gene coexpression network pattern across the lifespan*

To "map" variation in gene expression of the *DCC* coexpression network in the PFC over the human lifespan, we used the BrainSpan gene-expression database and compared postmortem data specific to the PFC from donors of various ages. We aggregated the data for childhood, adolescence and adulthood and calculated correlation matrices, presenting them with retained gene order (Fig. 1). The network's coexpression pattern is dynamic across postnatal ages. During childhood there was robust synchrony of gene activity. In

adolescence, when the PFC undergoes substantial maturation, the correlation matrix of genes coexpressed with *DCC* showed no clear structure. By adulthood, gene expression appeared to concentrate into specific hubs of activity.

DCC *ePRS predicted individual differences in brain size*

As shown in Table 1 and Table 2, the participant demographics for the MAVAN and UCI cohorts were relatively homogeneous, showing no differences between the low and high ePRS groups with respect to the confounders ($p > 0.05$).

We then sought to understand how the *DCC* coexpression network in the PFC is associated with total brain volume. We found a significant positive association between the ePRS and total brain volume (grey and white matter) among the children in MAVAN cohort ($\beta = 0.212$, $p = 0.043$; $n = 88$): participants with a higher *DCC* ePRS tended to have a larger brain volume (Fig. 2A).

We replicated this result in the UCI cohort. Similar to the MAVAN cohort, the UCI cohort ($n = 80$) showed a significant association between *DCC* ePRS and newborn total brain volume (grey and white matter, adjusted by intracranial volume; $\beta = 0.101$, $p = 0.048$; Fig. 2B). These findings provided evidence that the *DCC* coexpression network predicts differences in brain morphology development.

Specificity of the ePRS

We investigated whether a conventional PRS[60,61] based on a genome-wide association study of brain volume[63] was associated with differences in brain volume in the cohort of the present study. We found no correlation between the PRS (for several p value thresholds) and brain volume in the MAVAN cohort (Table 3). The *DCC* ePRS was not only more biologically meaningful than the conventional PRS,
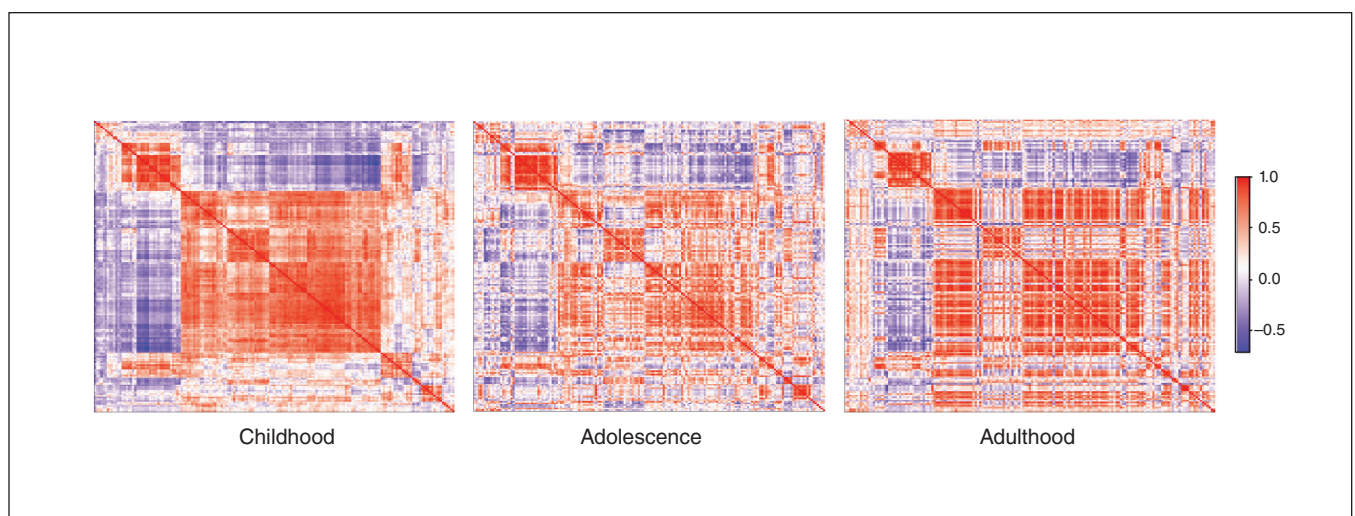

Fig. 1: Using an Euclidean matrix, we show coexpression levels of the *DCC* gene network in the prefrontal cortex through 3 life stages (red = positive coexpression correlation; purple = inverse coexpression correlation; white = no correlation). The order of genes in the network has been retained for the different life stages. As indicated by large clusters of same-direction expression (red and purple), the network's coexpression pattern has robust synchrony of gene activity, with notable clustering of the pattern as age increases.

but also sensitive to predicting volumetric brain differences in community-based samples of children.

The DCC coexpression network in the PFC comprises genes involved in mRNA translation

To examine the functional ontology of the genes that comprised the *DCC* coexpression network in the PFC, we screened for functional networks. Predominant enrichment was for the mRNA translation initiation and termination processes (Fig. 3). Gene ontology processes included cell adhesion, immune and inflammation functional networks, and Notch signalling.

Discussion

We generated an ePRS to determine whether variations in the function of the *DCC* gene network in the PFC predicted total brain volume in children. The *DCC* ePRS for the PFC was positively associated with brain volume in 2 separate community-based samples and was a stronger predictor than a conventionally computed PRS. Genes comprising the score are involved in cell function maintenance, and their activity in the PFC during childhood, adolescence and adulthood provide a snapshot of their dynamic recruitment throughout the lifespan.

The DCC receptors are implicated in the organization of long-distance axonal wiring across early life and adolescence.[10,15,66,67] In humans, bialleic loss-of-function mutations in the *DCC* gene lead to broad disorganization of white matter tracts, developmental split-brain syndrome and cognitive deficits.[68,69] People who are *DCC*-haploinsufficient exhibit morphological and connectivity alterations, including mesocorticolimbic connectivity and volumetric alterations.[19,20] The DCC receptors have been shown to play a critical role in PFC development.[10,11,13,15,34,43,70] Our findings linking the *DCC* coexpression network in the PFC to total brain volume during normative childhood development suggests that early postnatal PFC maturation influences brain-wide development. It is also likely that similar *DCC* gene networks are expressed throughout the brain regions, coordinating both local and overall neuronal networks.

The effect size between the *DCC* ePRS for the PFC and total brain volume is likely to be reflected in behavioural outcomes and vulnerability to psychiatric disorders. Brain volume is associated with intrinsic brain activity[71] and implicated in cognitive outcomes, including educational attainment and intelligence.[72,73] Furthermore, brain volume is associated with psychiatric conditions such as autism spectrum disorder,[74–76] schizophrenia[77,78] and depression.[79–81] In forthcoming studies, we will assess whether the *DCC*

Table 1: Participant characteristics, MAVAN*

Characteristics	Total (n = 73)	Low ePRS (n = 39)	High ePRS (n = 34)	p value†
Male, n (%)	35 (47.9)	20 (51.3)	15 (44.1)	0.54
Age at scan, yr	9.27 ± 1.46	9.35 ± 1.41	9.17 ± 1.53	0.60
Gestational age, wk	39.18 ± 1.18	39.03 ± 1.16	39.35 ± 1.20	0.24
Birth weight, g	3265 ± 476	3223 ± 429	3314 ± 527	0.42
Breastfeeding duration, mo	7.37 ± 4.88	6.96 ± 4.79	7.81 ± 5.01	0.46
Smoking during pregnancy, n (%)	13 (18.1)	6 (15.8)	7 (20.6)	0.60
Maternal education, university degree or above, n (%)	38 (52.1)	20 (51.3)	18 (52.9)	0.89
Low income, n (%)	11 (16.9)	5 (13.9)	6 (20.7)	0.47

ePRS = expression-based polygenic risk score; MAVAN = Maternal Adversity, Vulnerability and Neurodevelopment.
*Data are presented as n (%) or mean ± standard deviation. Percentages were calculated based on the available data; for smoking during pregnancy, total n = 72, and for low income, total n = 65.
†We found no significant differences between children in the low and high ePRS groups.

Table 2: Participant characteristics, replication cohort (UCI)*

Characteristics	Total (n = 80)	Low ePRS (n = 44)	High ePRS (n = 36)	p value†
Male, n (%)	48 (60.0)	26 (59.1)	22 (61.1)	0.86
Corrected age at scan, d	21.08 ± 14.79	21.39 ± 16.27	20.69 ± 12.95	0.84
Gestational age, wk	39.18 ± 1.49	39.15 ± 1.67	39.22 ± 1.26	0.83
Birth weight, g	3336 ± 507	3361 ± 554	3305 ± 450	0.62
Breastfeeding duration, mo	6.41 ± 5.07	5.37 ± 4.89	7.7 ± 5.09	0.07
Smoking during pregnancy, n (%)	6 (7.5)	3 (6.8)	3 (8.3)	0.77
Maternal education, university degree or above, n (%)	27 (33.8)	12 (27.2)	15 (41.6)	0.13
Household income < $29 999/yr	26 (32.5)	14 (31.8)	12 (33.3)	0.28

ePRS = expression-based polygenic risk score; UCI = University of California, Irvine.
*Data are presented as n (%) or mean ± standard deviation. Percentages were calculated based on the available data.
†We found no significant differences between children in the low and high ePRS groups.

ePRS differs between healthy people and those vulnerable to mental illness.

The biological processes modulated by genes in the *DCC* network include mRNA translation, cell adhesion, particle transportation and inflammation. Based on the large clusters of genetic activity during childhood that we observed in the expression matrix and in the gene ontology analysis, it is likely that at this early age, the gene network regulates cellu-

lar fate and neural proliferation events. This idea is consistent with a recent analysis of genetic signatures of the human brain showing *DCC* among top 10% of genes with a consistent transcriptional regulation pattern across 132 different brain structures.[82] The *DCC* coexpression network is most likely part of a core network that modulates biological processes across the entire brain and, according to our gene-expression profile matrices across different life stages, remains dynamically active into adulthood.

The different *DCC* network expression patterns we observed in the childhood, adolescent and adult matrices suggest continuous recruitment and pruning of the network. Particularly interesting was the widespread reduction of synchronous gene expression during adolescence, which most likely accounts for individual-based experience, and shapes the function of the network into adulthood. The importance of changes in coexpression patterning across ages can be inferred from rodent studies showing that the function of DCC receptors vary according to maturational stage. During prenatal and early postnatal development, DCC is involved in myriad processes across the central nervous system, from driving the migration of neural-crest-derived cells[83] and participating in fetal telencephalic cortical plate development,[67] to guiding the growth of corticospinal tract axons[84,85] and retinal ganglion cell axons.[86] From juvenile age to adolescence, the role of the DCC receptors appears to become more specialized, as they are primarily involved in controlling the

Table 3: Conventional PRS association with total brain volume*

p value thresholds	β	*p* value	SNP count
PRS τ 0.0001	−0.113	0.31	2493
PRS τ 0.001	−0.055	0.61	6764
PRS τ 0.01	−0.184	0.12	23929
PRS τ 0.05	−0.145	0.24	65567
PRS τ 0.1	−0.189	0.13	103097
PRS τ 0.2	−0.151	0.25	161534
PRS τ 0.3	−0.144	0.28	208446
PRS τ 0.4	−0.152	0.25	248433
PRS τ 0.5	−0.156	0.24	282935

GWAS = genome-wide association studies; MAVAN = Maternal Adversity, Vulnerability and Neurodevelopment. PRS = polygenic risk score; SNP = single nucleotide polymorphism.
*Association between PRSs using the GWAS for total brain volume[63] and total brain volume in MAVAN children, with different PRS *p* value thresholds. We adjusted the regression models using the principal components of age, sex, site and population stratification.
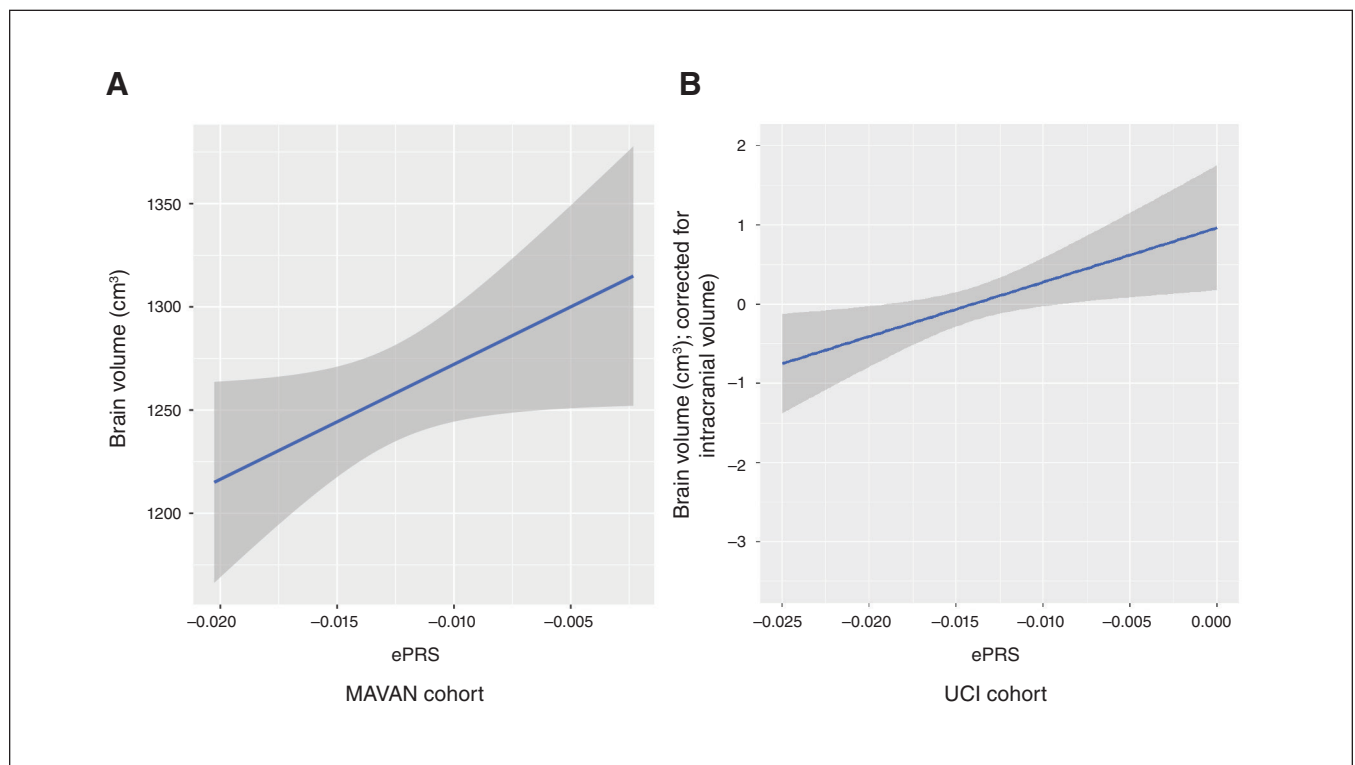

Fig. 2: Morphological differences predicted by *DCC* expression-based polygenic risk score (ePRS). In (A) the Maternal Adversity, Vulnerability and Neurodevelopment (MAVAN) cohort and (B) the University of California, Irvine (UCI) replication cohort, higher ePRS is associated with larger total brain volume.

targeting decisions of dopamine axons in limbic regions and organizing their connectivity in local circuitries.[10,15,70] In adulthood, DCC receptors are involved in axonal sprouting, maintenance of already established synaptic connections and synaptic plasticity via the recruitment of nascent or immature synapses.[87–92] The *DCC* coexpression network in the PFC may be involved in maintaining proliferative functions and establishing early global connections in childhood; fine-tuning network connectivity in adolescence; and maintaining local synaptic connectivity and function in adulthood.

Limitations

A limiting factor in this study was sample size.[93] Because MRI data collection is challenging in young participants, the final number of processed imaging scans was small. However, the fact that our findings were replicated in a second community-based child cohort counteracts this limitation. It is important to note that only few child cohorts with neuroimaging and genotype data are available, and consistency in age between cohorts is difficult to achieve. The sample size of the gene-expression data from BrainSpan that we used to create the developmental period-specific gene-expression matrices was relatively small, limiting the interpretation of this result.

The use of brain volume as a phenotype has benefits and limitations. In this study, the use of total brain volume al-

lowed us to obtain a glimpse at global morphological differences according to the child's ePRS. The population sample was that of a community cohort, so the variation in brain volume among individuals was expected to correspond to that observed in a healthy population. A higher association is likely to be identified in people with altered neurodevelopment. Using a gross measure such as total brain volume might mask some associations in which developmental alterations are restricted to particular circuits. As well, our analysis did not discern between histological features such as the ratio of neurons to glia, which can relate to variations in brain volume.

Conclusion

This study paves the path for research aimed at uncovering the pathways that underlie brain characteristics associated with psychiatric conditions. Coexpression gene networks provide information on biological processes. The *DCC* gene is an emerging hub gene associated with psychiatric illness, but the molecular pathways linking *DCC* dysfunction to pathological outcomes are only beginning to be elucidated. Our findings show that a network of genes coexpressed with *DCC* in the PFC and involved in basic cellular functions is associated with the development of brain volume and highlight the dynamic nature of the genetic contribution to brain development.
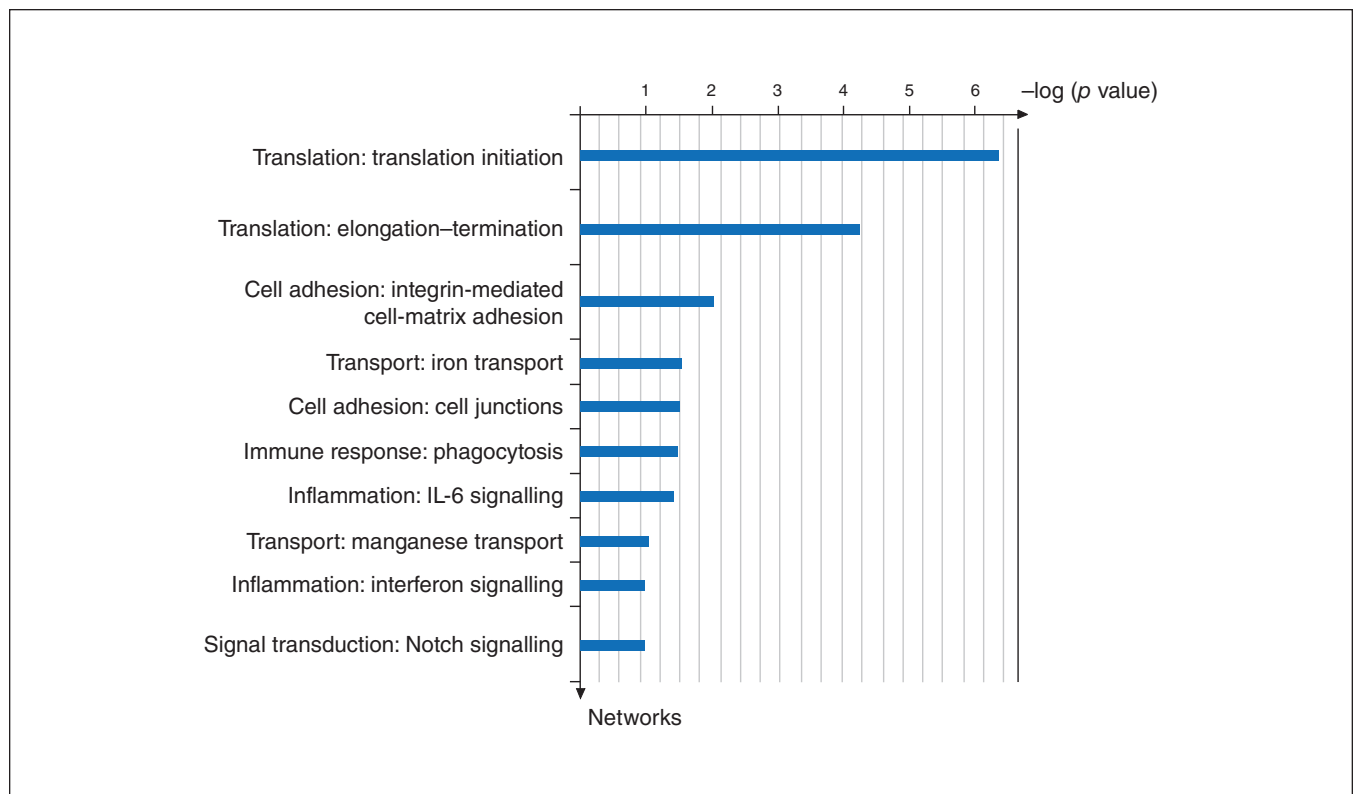

Fig. 3: Using Metacore software, we analyzed the coexpression gene list for networks that depict main associations (top 10) with particular cellular processes. The *y*-axis shows the order of the networks by significance. IL-6 = interleukin-6.

References

1. Fuster J. *The prefrontal cortex.* Cambridge (MA): Academic Press; 2015.
2. Gogtay N, Giedd JN, Lusk L, et al. Dynamic mapping of human cortical development during childhood through early adulthood. *Proc Natl Acad Sci U S A* 2004;101:8174-9.
3. Luna B. Developmental changes in cognitive control through adolescence. *Adv Child Dev Behav* 2009;37:233-78.
4. Sturman DA, Moghaddam B. The neurobiology of adolescence: changes in brain architecture, functional dynamics, and behavioral tendencies. *Neurosci Biobehav Rev* 2011;35:1704-12.
5. Ordaz SJ, Foran W, Velanova K, et al. Longitudinal growth curves of brain function underlying inhibitory control through adolescence. *J Neurosci* 2013;33:18109-24.
6. Larsen B, Luna B. Adolescence as a neurobiological critical period for the development of higher-order cognition. *Neurosci Biobehav Rev* 2018;94:179-95.
7. Kalsbeek A, Voorn P, Buijs RM, et al. Development of the dopaminergic innervation in the prefrontal cortex of the rat. *J Comp Neurol* 1988;269:58-72.
8. Naneix F, Marchand AR, Di Scala G, et al. Parallel maturation of goal-directed behavior and dopaminergic systems during adolescence. *J Neurosci* 2012;32:16223-32.
9. Willing J, Cortes LR, Brodsky JM, et al. Innervation of the medial prefrontal cortex by tyrosine hydroxylase immunoreactive fibers during adolescence in male and female rats. *Dev Psychobiol* 2017;59:583-9.
10. Reynolds LM, Pokinko M, Torres-Berrío A, et al. DCC receptors drive prefrontal cortex maturation by determining dopamine axon targeting in adolescence. *Biol Psychiatry* 2018;83:181-92.
11. Hoops D, Flores C. Making dopamine connections in adolescence. *Trends Neurosci* 2017;40:709-19.
12. Cuesta S, Nouel D, Reynolds LM, et al. Dopamine axon targeting in the nucleus accumbens in adolescence requires netrin-1. *Front Cell Dev Biol* 2020;8:487.
13. Grant A, Hoops D, Labelle-Dumais C, et al. Netrin-1 receptor-deficient mice show enhanced mesocortical dopamine transmission and blunted behavioural responses to amphetamine. *Eur J Neurosci* 2007;26:3215-28.
14. Flores C. Role of netrin-1 in the organization and function of the mesocorticolimbic dopamine system. *J Psychiatry Neurosci* 2011;36:296.
15. Manitt C, Eng C, Pokinko M, et al. DCC orchestrates the development of the prefrontal cortex during adolescence and is altered in psychiatric patients. *Transl Psychiatry* 2013;3:e338.
16. Pokinko M, Moquin L, Torres-Berrío A, et al. Resilience to amphetamine in mouse models of netrin-1 haploinsufficiency: role of mesocortical dopamine. *Psychopharmacology (Berl)* 2015;232:3719-29.
17. Torres-Berrío A, Lopez JP, Bagot RC, et al. DCC confers susceptibility to depression-like behaviors in humans and mice and is regulated by miR-218. *Biol Psychiatry* 2017;81:306-15.
18. Reynolds LM, Flores C. Guidance cues: linking drug use in adolescence with psychiatric disorders. *Neuropsychopharmacology* 2019;44:225.
19. Vosberg DE, Zhang Y, Menegaux A, et al. Mesocorticolimbic connectivity and volumetric alterations in DCC mutation carriers. *J Neurosci* 2018;38:4655-65.
20. Vosberg DE, Beaulé V, Torres-Berrío A, et al. Neural function in DCC mutation carriers with and without mirror movements. *Ann Neurol* 2019;85:433-42.
21. Vosberg DE, Leyton M, Flores C. The Netrin-1/DCC guidance system: dopamine pathway maturation and psychiatric disorders emerging in adolescence. *Mol Psychiatry* 2020;25:297-307.
22. Dunn EC, Wiste A, Radmanesh F, et al. Genome-wide association study (GWAS) and genome-wide by environment interaction study (GWEIS) of depressive symptoms in African American and Hispanic/Latina women. *Depress Anxiety* 2016;33:265-80.
23. Okbay A, Baselmans BM, De Neve JE, et al. Genetic variants associated with subjective well-being, depressive symptoms, and neuroticism identified through genome-wide analyses. *Nat Genet* 2016;48:624-33.
24. Smith DJ, Escott-Price V, Davies G, et al. Genome-wide analysis of over 106 000 individuals identifies 9 neuroticism-associated loci. *Mol Psychiatry* 2016;21:749-57.
25. Zeng Y, Navarro P, Fernandez-Pujals AM, et al. A combined pathway and regional heritability analysis indicates NETRIN1 pathway is associated with major depressive disorder. *Biol Psychiatry* 2017;81:336-46.
26. Ward J, Strawbridge RJ, Bailey ME, et al. Genome-wide analysis in UK Biobank identifies four loci associated with mood instability and genetic correlation with major depressive disorder, anxiety disorder and schizophrenia. *Transl Psychiatry* 2017;7:1264.

27. Roberson-Nay R, Wolen AR, Lapato DM, et al. Twin study of early-onset major depression finds DNA methylation enrichment for neurodevelopmental genes. *bioRxiv* 2018;422345. Available: https://doi.org/10.1101/422345 (accessed 2020 Nov. 4).

28. Aberg KA, Shabalin AA, Chan RF, et al. Convergence of evidence from a methylome-wide CpG-SNP association study and GWAS of major depressive disorder. *Transl Psychiatry* 2018;8:162.

29. Barbu MC, Zeng Y, Shen X, et al. Association of whole-genome and NETRIN1 signaling pathway-derived polygenic risk scores for major depressive disorder and thalamic radiation white matter microstructure in UK Biobank. *Biol Psychiatry Cogn Neurosci Neuroimaging* 2019;4:91-100.

30. Leday GG, Vértes PE, Richardson S, et al. Replicable and coupled changes in innate and adaptive immune gene expression in two case-control studies of blood microarrays in major depressive disorder. *Biol Psychiatry* 2018;83:70-80.

31. Wray NR, Ripke S, Mattheisen M, et al. Genome-wide association analyses identify 44 risk variants and refine the genetic architecture of major depression. *Nat Genet* 2018;50:668-81.

32. Arnau-Soler A, Macdonald-Dunlop E, Adams MJ, et al. Genome-wide by environment interaction studies of depressive symptoms and psychosocial stress in UK Biobank and Generation Scotland. *Transl Psychiatry* 2019;9:14.

33. Strawbridge RJ, Ward J, Ferguson A, et al. Identification of novel genome-wide associations for suicidality in UK Biobank, genetic correlation with psychiatric disorders and polygenic association with completed suicide. *EBioMedicine* 2019;41:517-25.

34. Lee PH, Anttila V, Won H, et al. Genomic relationships, novel loci, and pleiotropic mechanisms across eight psychiatric disorders. *Cell* 2019;179:1469-82.

35. Torres-Berrío A, Hernandez G, Nestler EJ, et al. The netrin-1/DCC guidance cue pathway as a molecular target in depression: translational evidence. *Biol Psychiatry* 2020;88:611-24.

36. Grant A, Fathalli F, Rouleau G, et al. Association between schizophrenia and genetic variation in DCC: a case–control study. *Schizophr Res* 2012;137:26-31.

37. Yan P, Qiao X, Wu H, et al. An association study between genetic polymorphisms in functional regions of five genes and the risk of schizophrenia. *J Mol Neurosci* 2016;59:366-75.

38. Smeland OB, Wang Y, Frei O, et al. Genetic overlap between schizophrenia and volumes of hippocampus, putamen, and intracranial volume indicates shared molecular genetic mechanisms. *Schizophr Bull* 2018;44:854-64.

39. Khadka S, Narayanan B, Meda SA, et al. Genetic association of impulsivity in young adults: a multivariate study. *Transl Psychiatry* 2014;4:e451.

40. Zanetti KA, Wang Z, Aldrich M, et al. Genome-wide association study confirms lung cancer susceptibility loci on chromosomes 5p15 and 15q25 in an African-American population. *Lung Cancer* 2016;98:33-42.

41. Kichaev G, Bhatia G, Loh P-R, et al. Leveraging polygenic functional enrichment to improve GWAS power. *Am J Hum Genet* 2019; 104:65-75.

42. Linnér RK, Biroli P, Kong E, et al. Genomewide association analyses of risk tolerance and risky behaviors in over 1 million individuals identify hundreds of loci and shared genetic influences. *Nat Genet* 2019;51:245-57.

43. Li HJ, Qu N, Hui L, et al. Further confirmation of netrin 1 receptor (DCC) as a depression risk gene via integrations of multi-omics data. *Transl Psychiatry* 2020;10:1-15.

44. O'Donnell KA, Gaudreau H, Colalillo S, et al. The Maternal Adversity Vulnerability and Neurodevelopment (MAVAN) project: theory and methodology. *Can J Psychiatry* 2014;59:497-508.

45. Moog NK, Entringer S, Rasmussen JM, et al. Intergenerational effect of maternal exposure to childhood maltreatment on newborn brain anatomy. *Biol Psychiatry* 2018;83:120-7.

46. Toepfer P, O'Donnell KJ, Entringer S, et al. A role of oxytocin receptor gene brain tissue expression quantitative trait locus rs237895 in the intergenerational transmission of the effects of maternal childhood maltreatment. *J Am Acad Child Adolesc Psychiatry* 2019;58:1207-1216.

47. McDaniel MA. Big-brained people are smarter: a meta-analysis of the relationship between in vivo brain volume and intelligence. *Intelligence* 2005;33:337-46.

48. Rapoport JL, Castellanos FX, Gogate N et al. Imaging normal and abnormal brain development: new perspectives for child psychiatry. *Aust N Z J Psychiatry* 2001;35:272-81.

49. Nave G, Jung WH, Linnér RK et al. Are bigger brains smarter? Evidence from a large-scale preregistered study. *Psychol Sci* 2019; 30:43-54.

50. Silveira PP, Pokhvisneva I, Parent C, et al. Cumulative prenatal exposure to adversity reveals associations with a broad range of neurodevelopmental outcomes that are moderated by a novel, biologically informed polygenetic score based on the serotonin transporter solute carrier family C6, member 4 (SLC6A4) gene expression. *Dev Psychopathol* 2017;29:1601-17.

51. Chang CC, Chow CC, Tellier LC, et al. Second-generation PLINK: rising to the challenge of larger and richer datasets. *Gigascience* 2015 4:7.

52. McCarthy S, Das S, Kretzschmar W, et al. A reference panel of 64,976 haplotypes for genotype imputation. *Nat Genet* 2016;48:1279-83.

53. Patterson N, Price AL, Reich D. Population structure and eigenanalysis. *PLoS Genet* 2006;2:e190.

54. Price AL, Patterson NJ, Plenge RM, et al. Principal components analysis corrects for stratification in genome-wide association studies. *Nat Genet* 2006;38:904-9.

55. Chakravarty MM, Steadman P, van Eede MC, et al. Performing label-fusion-based segmentation using multiple automatically generated templates. *Hum Brain Mapp* 2013;34:2635-54.

56. Pipitone J, Park MTM, Winterburn J, et al. Multi-atlas segmentation of the whole hippocampus and subfields using multiple automatically generated templates. *Neuroimage* 2014;101:494-512.

57. Cherel M, Budin F, Prastawa M, et al. Automatic tissue segmentation of neonate brain MR Images with subject-specific atlases. In: *SPIE conference proceedings, vol. 9413: medical imaging 2015: image processing*; 2015; Orlando (FL). Bellingham (WA): SPIE; 2015:941311. Available: www.spiedigitallibrary.org/conference-proceedings-of-spie/browse/spie-medical-imaging/2015 (accessed 2020 Nov. 12).

58. Hari Dass SA, McCracken K, Pokhvisneva I, et al. A biologically informed polygenic score identifies endophenotypes and clinical conditions associated with the insulin receptor function on specific brain regions. *EBioMedicine* 2019;42:188-202.

59. Galili T, O'Callaghan A, Sidi J, et al. heatmaply: an R package for creating interactive cluster heatmaps for online publishing. *Bioinformatics* 2018;34:1600-2.

60. Wray NR, Goddard ME. Multi-locus models of genetic risk of disease. *Genome Med* 2010;2:10.

61. Wray NR, Lee SH, Mehta D, et al. Research review: polygenic methods and their application to psychiatric traits. *J Child Psychol Psychiatry* 2014;55:1068-87.

62. Chen LM, Yao N, Garg E, et al. PRS-on-Spark (PRSoS): a novel, efficient and flexible approach for generating polygenic risk scores. *BMC Bioinformatics* 2018;19:295.

63. Jansen PR, Nagel M, Watanabe K et al. GWAS of brain volume on 54407 individuals and cross-trait analysis with intelligence identifies shared genomic loci and genes. *bioRxiv* 2019;613489. Available: https://doi.org/10.1101/613489 (accessed 2020 Nov. 4).

64. Kramer MS, Platt R, Yang H, et al. Are all growth-restricted newborns created equal(ly)? *Pediatrics* 1999;103:599-602.

65. Villar J, Cheikh IL, Victora CG, et al. International standards for newborn weight, length, and head circumference by gestational age and sex: the Newborn Cross-Sectional Study of the INTER-GROWTH-21st Project. *Lancet* 2014;384:857-68.

66. Livesey FJ, Hunt SP. Netrin and netrin receptor expression in the embryonic mammalian nervous system suggests roles in retinal, striatal, nigral, and cerebellar development. *Mol Cell Neurosci* 1997;8:417-29.

67. Harter PN, Bunz B, Dietz K, et al. Spatio-temporal deleted in colorectal cancer (DCC) and netrin-1 expression in human foetal brain development. *Neuropathol Appl Neurobiol* 2010;36:623-35.

68. Jamuar SS, Schmitz-Abe K, D'Gama AM, et al. Biallelic mutations in human DCC cause developmental split-brain syndrome. *Nat Genet* 2017;49:606.

69. Marsh AP, Edwards TJ, Galea C, et al. DCC mutation update: congenital mirror movements, isolated agenesis of the corpus callosum, and developmental split brain syndrome. *Hum Mutat* 2018;39:23-39.

70. Hoops D, Reynolds LM, Restrepo-Lozano JM, et al. Dopamine development in the mouse orbital prefrontal cortex is protracted and sensitive to amphetamine in adolescence. *eNeuro* 2018;5:ENEURO.0372-17.

71. Qing Z, Gong G. Size matters to function: brain volume correlates with intrinsic brain activity across healthy individuals. *Neuroimage* 2016;139:271-8.
72. Alemany S, Jansen PR, Muetzel RL, et al. Common polygenic variations for psychiatric disorders and cognition in relation to brain morphology in the general pediatric population. *J Am Acad Child Adolesc Psychiatry* 2019;58:600-7.
73. Cox SR, Ritchie SJ, Fawns-Ritchie C, et al. Structural brain imaging correlates of general intelligence in UK Biobank. *Intelligence* 2019; 76:101376.
74. Nordahl CW, Lange N, Li DD, et al. Brain enlargement is associated with regression in preschool-age boys with autism spectrum disorders. *Proc Natl Acad Sci U S A* 2011;108:20195-200.
75. Sacco R, Gabriele S, Persico AM. Head circumference and brain size in autism spectrum disorder: a systematic review and meta-analysis. *Psychiatry Res Neuroimaging* 2015;234:239-51.
76. Hazlett HC, Gu H, Munsell BC, et al. Early brain development in infants at high risk for autism spectrum disorder. *Nature* 2017; 542:348-51.
77. Mehler C, Warnke A. Structural brain abnormalities specific to childhood-onset schizophrenia identified by neuroimaging techniques. *J Neural Transm (Vienna)* 2002;109:219-34.
78. Steen RG, Mull C, Mcclure R, et al. Brain volume in first-episode schizophrenia: systematic review and meta-analysis of magnetic resonance imaging studies. *Br J Psychiatry* 2006;188:510-8.
79. Steingard RJ, Renshaw PF, Hennen J, et al. Smaller frontal lobe white matter volumes in depressed adolescents. *Biol Psychiatry* 2002;52:413-7.
80. Phillips JL, Batten LA, Aldosary F, et al. Brain-volume increase with sustained remission in patients with treatment-resistant unipolar depression. *J Clin Psychiatry* 2012;73:625-31.
81. Pagliaccio D, Alqueza KL, Marsh R, et al. Brain volume abnormalities in youth at high risk for depression: adolescent brain and cognitive development study. *J Am Acad Child Adolesc Psychiatry* 2019.
82. Hawrylycz M, Miller JA, Menon V, et al. Canonical genetic signatures of the adult human brain. *Nat Neurosci* 2015;18:1832.
83. Jiang Y, Liu MT, Gershon MD. Netrins and DCC in the guidance of migrating neural crest-derived cells in the developing bowel and pancreas. *Dev Biol* 2003;258:364-84.
84. Finger JH, Bronson RT, Harris B, et al. The netrin 1 receptors Unc5h3 and Dcc are necessary at multiple choice points for the guidance of corticospinal tract axons. *J Neurosci* 2002;22: 10346-56.
85. Furne C, Rama N, Corset V, et al. Netrin-1 is a survival factor during commissural neuron navigation. *Proc Natl Acad Sci U S A* 2008; 105:14465-70.
86. Deiner MS, Kennedy TE, Fazeli A, et al. Netrin-1 and DCC mediate axon guidance locally at the optic disc: loss of function leads to optic nerve hypoplasia. *Neuron* 1997;19:575-89.
87. Goldman JS, Ashour MA, Magdesian MH, et al. Netrin-1 promotes excitatory synaptogenesis between cortical neurons by initiating synapse assembly. *J Neurosci* 2013;33:17278-89.
88. Horn KE, Glasgow SD, Gobert D, et al. DCC expression by neurons regulates synaptic plasticity in the adult brain. *Cell Rep* 2013;3:173-85.
89. Glasgow, S. D., Wong, E. W., Thompson-Steckel, G., et al. Pre- and post-synaptic roles for DCC in memory consolidation in the adult mouse hippocampus. *Mol Brain 2020*;13:56.
90. Manitt C, Nikolakopoulou AM, Almario DR, et al. Netrin participates in the development of retinotectal synaptic connectivity by modulating axon arborization and synapse formation in the developing brain. *J Neurosci* 2009;29:11065-77.
91. Muramatsu R, Nakahara S, Ichikawa J, et al. The ratio of "deleted in colorectal cancer" to "uncoordinated-5A" netrin-1 receptors on the growth cone regulates mossy fibre directionality. *Brain* 2010; 133:60-75.
92. Yetnikoff L, Eng C, Benning S, et al. Netrin-1 receptor in the ventral tegmental area is required for sensitization to amphetamine. *Eur J Neurosci* 2010;31:1292-302.
93. Steen RG, Hamer RM, Lieberman JA. Measuring brain volume by MR imaging: impact of measurement precision and natural variation on sample size requirements. *AJNR Am J Neuroradiol* 2007;28:1119-25.